

Treatment and Degradation of Azo Dye Waste Industry by Electro-Fenton Process

A. Wakrim^{a,*}, Z. Zaroual^a, S. El Ghachtouli^a, J. Jamal Eddine^b and M. Azzi^a

^aLaboratory Interface Materials Environment, Department of Chemistry, Faculty of Sciences Ain Chock, B.P 5366 Maarif Casablanca, Morocco

^bLaboratory of Synthesis, Extraction and Physico-chemical Study of Organic Molecules, Department of Chemistry, Faculty of Sciences Ain Chock, B.P 5366 Maarif Casablanca, Morocco

(Received 21 November 2021, Accepted 22 March 2022)

The Electro-Fenton technique was used to investigate the discoloration of carmoisine red azo dye solution. Carbon graphite (cathode) and platinum (anode) electrodes were used to achieve optimal discoloration efficiency. We examined the effect of Fe^{2+} concentration and current density. The results showed that with 200 mA cm^{-2} of electrolysis current and 0.2 mM of Fe^{2+} at $\text{pH} = 3$; 93% discoloration efficiency was achieved in 60 min. IR, LC-MS-MS, and Ion Chromatography studies were used to evaluate the degradation process of carmoisine red. Intermediates of aromatic compounds have been identified. A possible carmoisine red degradation pathway was proposed and discussed.

Keywords: Electrode material, Azo dye, Electro-Fenton process, Discoloration, Degradation

INTRODUCTION

Azo dyes are a type of synthetic dye that combines an azo functional group ($-\text{N}=\text{N}-$) and aromatic groups to produce a variety of colors [1,2].

According to several studies, there are over 100,000 commercially available dyes, with an annual production of about 7×10^5 tons of dye-stuff [3]. They're widely employed in a variety of industries, including textiles, paper, printing, dye, pharmaceuticals, food, cosmetics, plastics, and electronics. They represented almost a third of the total dye markets [4-6]. After being used in an industrial process, the majority of azo dyes were discharged into the environment. Because they are toxic, carcinogenic, mutagenic, and allergenic, causing human genes are changed [7], releasing them into the environment has resulted in a lot of harmful effects on the ecosystems [8-11].

This dye is not very hazardous but can cause harmful effects and in extreme conditions can cause increased heart rate, vomiting, severe seizures, cyanosis, jaundice,

quadriplegia, and necrosis in humans. In addition, prolonged exposure to this dye may damage the mucous membrane and the digestive tract [12,13].

To avoid polluting the environment, research efforts were needed to create robust and effective oxidation methods to remove these pollutants and their byproducts from wastewaters.

Biochemical and coagulation techniques have traditionally been used to treat solutions containing soluble dyes. All of these procedures are either expensive, inefficient or result in the creation of secondary harmful waste. Advanced oxidation technologies, as an alternative to traditional methods, have gained popularity in recent years (AOPs).

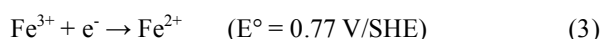
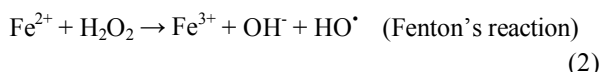
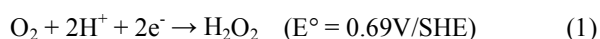
Advanced oxidation processes (AOPs) are strong chemical, photochemical, photocatalytic, and electrochemical processes that use the hydroxyl radical ($\bullet\text{OH}$) as a powerful oxidant to degrade toxic and/or biorefractory organics in wastewaters [4,14]. The high standard reduction potential of $\bullet\text{OH}$ ($E^\circ (\bullet\text{OH}/\text{H}_2\text{O}) = 2.80 \text{ V/SHE}$) makes possible its non-selective reaction with most organics yielding dehydrogenated or hydroxylated

*Corresponding author. E-mail: asmaa.wakrim@gmail.com

derivatives, which can be in turn completely mineralized.

Electro-Fenton process is one of the advanced oxidation processes (AOPs) [15], that involves creating Fenton's reagent ($\text{Fe}^{2+}/\text{H}_2\text{O}_2$) in an acidic medium ($\text{pH} = 3$) at the cathode by O_2 reduction (Eq. (1)) [16,17].

The electro-generated H_2O_2 interacts with the added Fe^{2+} ions to form hydroxyl radicals HO^\bullet (Eq. (2)). The cathodic reduction of Fe^{3+} ions is mainly responsible for the regeneration of Fe^{2+} ions (Eq. (3)). As a result, only a small amount of iron (Fe^{2+}) catalyst is required.



The hydroxyl radical obtained can be used to effectively degrade organic pollutants [18,19]. This method is a good alternative to the whole decomposition of hazardous substances for environmental and ecosystem protection since it is a quick and inexpensive process that does not require the use of toxic chemicals.

In the present work, we used the Electro-Fenton process with a Pt anode and a graphite carbon cathode to explore the discoloration of the azo dye carmoisine red in aqueous solutions. To achieve an optimal condition of dye degradation, many treatment parameters such as Fe^{2+} concentration and electrolysis current have been investigated. Infrared Spectroscopy, liquid chromatography-mass spectrometry (LC-MS-MS), and ion chromatography (IC) were used to examine the intermediate products generated during the treatment of carmoisine red solution. Based on these results, a plausible mechanism pathway of the degradation of carmoisine dye was proposed.

MATERIALS AND METHODS

Chemicals

The synthetic organic dye used was carmoisine red. Ferrous sulphate heptahydrate ($\text{FeSO}_4 \cdot 7\text{H}_2\text{O}$), sodium sulfate (Na_2SO_4), and Sulphuric acid (H_2SO_4) were all reagent grades and utilized without additional purification. All of the solutions were made with distilled water, and the

tests were carried out at room temperature. A HANNA HI8519N pH meter was used to determine the pH.

Electrochemical Cell and Apparatus

Degradation of carmoisine red by the Electro-Fenton process was performed in an undivided electrochemical cell equipped with two electrodes (Fig. 1).

The cathode material was a graphite carbon 3 cm^2 and the anode material was a platinum 14 cm^2 . The applied current between these electrodes was performed by a Potentiostat VoltaLab type PGZ 100. Prior to the electrolysis, compressed air was bubbled through the solution to reach a stationary O_2 concentration. A concentration of sodium sulfate 1 M (Na_2SO_4) was added to the solution as the supporting electrolyte. The iron sulfate ($\text{FeSO}_4 \cdot 7\text{H}_2\text{O}$) catalyzing the Fenton reaction was added to the reaction medium before the beginning of the electrolysis. The pH of the solutions was adjusted to 3 by sulphuric acid (1 M) under stirring to avoid the precipitation of ferric hydroxides. The initial concentration of carmoisine dye used in this study was 1 g l^{-1} . The spectrophotometric measurements were carried out at $\lambda = 515\text{ nm}$ using a Helios gamma spectrophotometer since the λ_{max} of the azo bond $\text{N}=\text{N}$ is around that wavelength.

Instruments and Analytical Procedures

Apparatus. The HPLC-MS-MS system consisted of a Shimadzu LCMS-8030 triple quadrupole mass spectrometer operating in the electrospray ionization (ESI) mode. The Shimadzu HPLC system was equipped with a degasser,

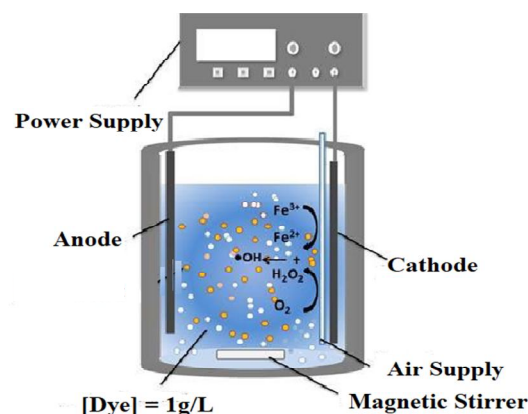


Fig. 1. Experimental set-up for Electro-Fenton experiments.

binary gradient pumps, a column oven, and an auto-sampler.

UPLC conditions: The degradation of carmoisine red was measured by high-performance liquid chromatography (HPLC) using Shim-pack GIST column C18 (2.1 × 100 mm). The mobile phase was Methanol: Water 60:40 (v/v), with isocratic elution at a flow rate of 0.3 ml min⁻¹. The column temperature was maintained at 25 °C. The injection volume was 10 µl. The detection was carried out at a wavelength of 220 nm.

Mass spectroscopy (MS) conditions: The following settings were used: the nebulizing gas and drying gas was nitrogen at a flow rate of 2 and 15 l min⁻¹, respectively. The interface voltage was set to 4.5 kV. The desolvation line (DL) temperature was 250 °C while the heat block temperature was 400 °C. The well time was set to 80 ms and detection was carried out within a mass range of 100-700 m/z.

Ion chromatography (IC). Ion chromatography (Metrohm 883 Basic IC plus) in combination with a conductivity detector was used to determine the concentration of anions (such as nitrate and sulphate ions) emitted during oxidation. The anionic exchanger column (6.1006.430 Metrosep A Supp 4) was used. The volume of injections was 10 µL. The mobile phase used was Na₂CO₃ (1.8 mM) and NaHCO₃ (1.7 mM).

Fourier transform infrared (FT-IR) spectroscopy. The powdered tablet samples were placed on Smart iTR™ Attenuated Total Reflectance (ATR) accessory composed of diamond crystal as sample handling technique at a controlled ambient temperature (25 °C). Samples were scanned using Nicolet iS10 FTIR spectrophotometer (Thermo Fisher Scientific). The instrument was connected to software OMNIC and spectra were scanned at wavenumbers of 4000-650 cm⁻¹, recorded for 32 scans at a resolution of 4 cm⁻¹. The air spectrum was used as background. Each data point was recorded in three replicates using absorbance mode to facilitate quantitative analysis.

RESULTS AND DISCUSSION

Discoloration of the Carmoisine Red Solution Using the Electro-Fenton Process

The study was carried out using a 1 g l⁻¹ synthetic

solution of carmoisine red dye. The UV-Vis spectrum of the solution was drawn and shown in Fig. 2. All experiments were performed in a 50 ml carmoisine red solution at 25 °C under magnetic stirring.

Effect of Fe²⁺ Concentration

The influence of Fe²⁺ concentration on the discoloration efficiency of carmoisine red solution using the Electro-Fenton process is shown in Fig. 3. Experiments were carried out with various concentrations of Fe²⁺ (from 0.05 to 0.6 mM), at a fixed electrolysis current density of 200 mA cm⁻² and pH = 3. The results are presented in Fig. 3.

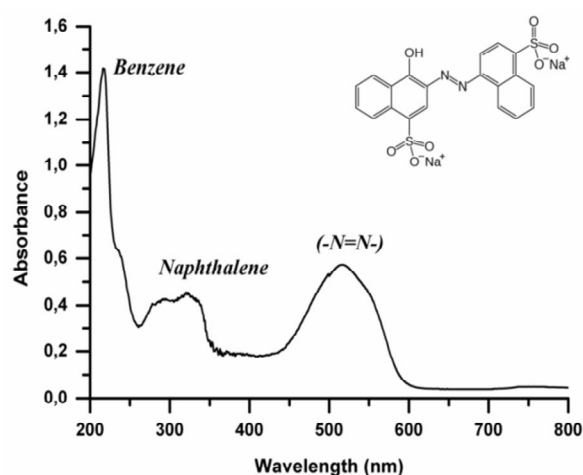


Fig. 2. The chemical structure and the UV-Vis spectrum of the carmoisine solution.

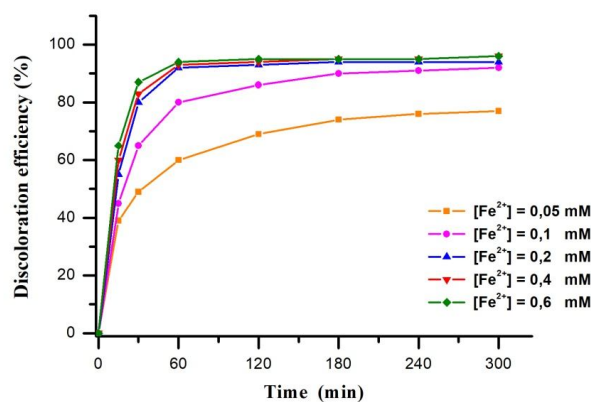


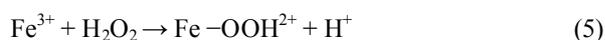
Fig. 3. Effect of Fe²⁺ concentration on the discoloration efficiency of carmoisine solution, [Dye] = 1 g l⁻¹; i = 200 mA cm⁻²; pH_i = 3; bubbled O₂.

The efficiency of discoloration is proportional to the initial concentration of ferrous iron, as shown in Fig. 3. When the Fe^{2+} concentration was increased, the discoloration efficiency increased. The Electro-Fenton process appeared to be most effective at Fe^{2+} concentration of 0.2 mM. Similar results have already been reported [20-23].

Indeed, the stabilization of carmoisine discoloration efficiency while the Fe^{2+} concentration increased can be explained by the presence of parasitic reactions that consume the hydroxyl radicals according to the reaction (4) [22]:



On the other hand, the Fe^{3+} ions generated could react with hydrogen peroxide H_2O_2 , according to reactions 5 and 6 [24]. This contributed to decrease discoloration efficiency.



Thus, the initial concentration of Fe^{2+} was a very influential parameter in the Electro-Fenton process. In all the following experiments the concentration of Fe^{2+} catalyst was fixed at 0.2 mM.

Effect of electrolysis current. After determining the catalyst concentration, the most suitable current density for carmoisine discoloration using the Electro-Fenton process should be established. Different solutions containing the same amount of carmoisine (1 g l^{-1}) were electrolyzed at different current densities ranging from 40 to 300 mA cm^{-2} for this purpose. Figure 4 shows the final results.

Figure 4 shows that the discoloration efficiency of carmoisine was improved when the electrolysis current was increased from 40 to 200 mA cm^{-2} . According to the reaction (2), this was due to a larger production of the Fenton reagent ($\text{Fe}^{2+}/\text{H}_2\text{O}_2$), which leads to a higher production of hydroxyl radicals [25]. We also observed that the discoloration efficiency remained constant for the electrolysis current $i = 300 \text{ mA cm}^{-2}$. It was almost similar to that obtained for $i = 200 \text{ mA cm}^{-2}$ after 60 min of

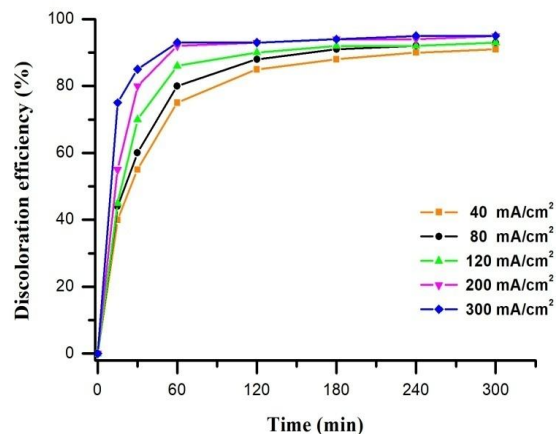


Fig. 4. Effect of electrolysis current on discoloration efficiency of carmoisine solution; $[\text{Dye}] = 1 \text{ g l}^{-1}$; $[\text{Fe}^{2+}] = 0.2 \text{ mM}$; $\text{pH}_i = 3$; bubbled O_2 .

electrolysis time. Furthermore, according to reaction (7), an excess of current favored the formation of H_2 at the cathode.



Similar observations were reported in other studies (Acid Orange 7) [23,26]. To summarize, increasing the electrolysis current can improve the efficiency of the Electro-Fenton process, but the value should be limited to 200 mA cm^{-2} to reduce energy cost.

Characterization of Carmoisine Red Solution after Degradation by the Electro-Fenton Process

Characterization by fourier transforms infrared spectroscopy (FT-IR). The IR spectra before and after treatment of the dye solution were generated and illustrated in Fig. 5 with the objective of understanding the carmoisine dye molecule behavior under the effect of the Electro-Fenton process.

Before treatment, the IR spectrum of carmoisine red solution revealed a broad and intense band at 3436 cm^{-1} , which was attributed to stretching vibrations of $-\text{OH}$ groups (Fig. 5 and Table 1) [27]. The band at 1620 cm^{-1} was assigned to aromatic $\text{C}=\text{O}$ stretching vibration [28,29]. The intense band at 1494 cm^{-1} was attributed to the azo bond of the dye ($-\text{N}=\text{N}-$) [29-31]. The band at 1181 cm^{-1} could be assigned to $\text{C}-\text{O}$ stretching vibrations [32]. The bands at

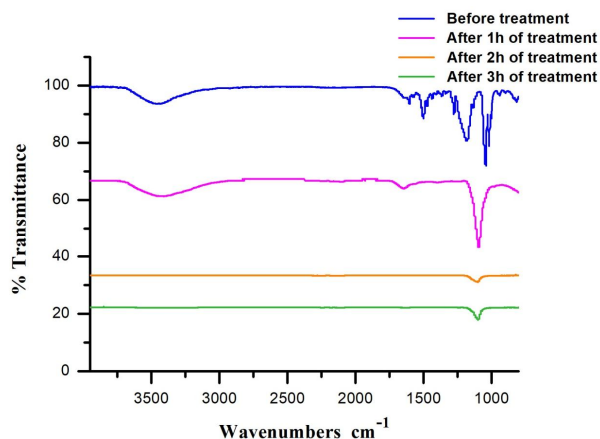


Fig. 5. IR spectra of carmoisine red solution before and after treatment by the Electro-Fenton process. [Dye] = 1 g l⁻¹, [Fe²⁺] = 0.2 mM, i = 200 mA cm⁻².

Table 1. IR Spectrum Band Assignments

Wavenumbers (cm ⁻¹)	Functional groups along with the mode of vibration
3436	Stretching vibration of hydrogen bonded (-OH)
1620	C=O
1494	-N=N-
1181	C-O
1043	C-C
940	
823	C-H
1003	-S=O

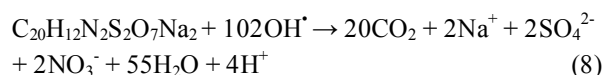
1043 and 940 cm⁻¹ corresponded to aromatic ring C-C stretching vibrations [31], while the bands at 823 cm⁻¹ could be ascribed to C-H stretching vibrations [32]. The absorption band near 1003 cm⁻¹ was attributed to the S=O bond [31,33].

The IR spectra after 1 h of solution treatment using the Electro-Fenton process is shown in Figure 5. We observed the disappearance of absorption bands at 1494, 1181, 1043, and 823 cm⁻¹. Also, the spectrum revealed the presence of three lower intensity bands at 3436, 1661, and 1124 cm⁻¹ which were attributed to the -OH, -C=O, and

-S=O groups, respectively [34,35].

After 2 and 3 h of treatment, we observed the disappearance of all the bands. A single low-intensity band at 1124 cm⁻¹ attributed to the deformation of the naphthalene and SO₃⁻ naphthalene groups [31].

Characterization of carmoisine red solution after treatment by ionic chromatography (IC). The total mineralization of organic compounds containing C, S, and N elements leads generally to the formation of carbon dioxide, sulphate, and nitrate compounds following the reaction (8).



Ionic chromatography was used to monitor the evolution of nitrate and sulphate ions concentrations during the Electro-Fenton oxidation process. Figures 6, 7, and Table 2 show the results.

The evolution of sulphate ions concentration during the Electro-Fenton treatment of carmoisine solution is presented in Fig. 7. After 5 h of electrolysis, the concentration of SO₄²⁻ ions formed from carmoisine degradation reached 340 g l⁻¹. This value was close to the theoretical value of 382 g l⁻¹ as displayed in Table 2, which showed that the sulphate ions release was almost 89%. This indicated that most of the (-SO₃⁻) group present in the carmoisine

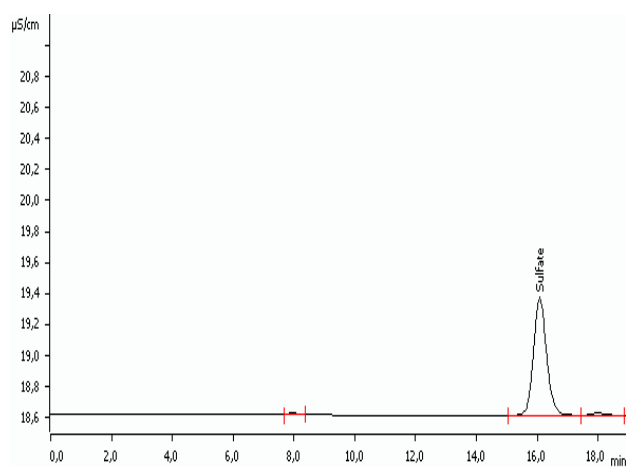


Fig. 6. Ionic chromatography spectrum after 60 min of solution treatment.

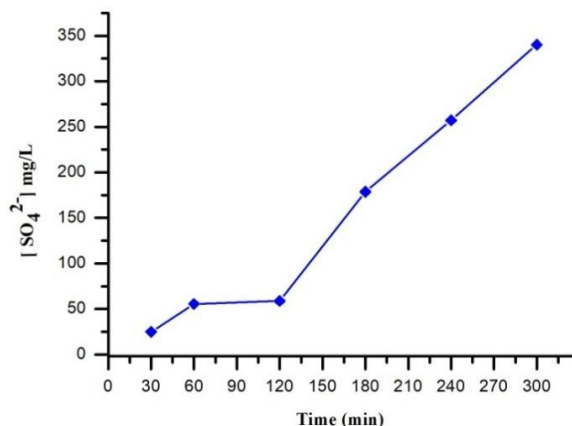


Fig. 7. Evolution of sulphate ions concentration during the Electro-Fenton treatment of carmoisine red solution.

Table 2. Inorganic Anions Concentration after 300 min of Solution Treatment

	[SO ₄ ²⁻] (mg l ⁻¹)	[NO ₃ ⁻] (mg l ⁻¹)
Maximum concentration for complete mineralization*	382	241
Experimental value (After 5 h of treatment)	340	0
Experimental value/Maximum value (%)	89%	0

*Calculated according to reaction (8).

structure was oxidized with the quantitative formation of SO₄²⁻ ion [11,36].

On the other hand, the ionic chromatography spectrum did not reveal the presence of nitrate ions in the solution after treatment (Fig. 6), this could be explained by the formation of gaseous molecules such as N_xO_y and more particularly NO₂ as reported for similar treatments of other azo dyes [14,35], or by the formation of nitrated organic intermediates [37,38].

Analysis of intermediates formed after degradation of carmoisine red solution by LC/MS/MS. Table 3 shows the retention times in the liquid chromatograms of various intermediates formed during the Electro-Fenton degradation

of carmoisine red. The components eluted with different retention times were subjected to mass spectrometry and identified by the interpretation of their fragment ions in the mass spectra. Figure 8 presents the mass spectra of the intermediates.

Table 3. Chemical Structures of Intermediates Identified by LC/MS/MS in Carmoisine Red Solution after Treatment

Intermediate number	(A)	(B)	(C)
Chemical structure			
m/z	355	328	102
R _t (min)	1.5	3.5	4.6

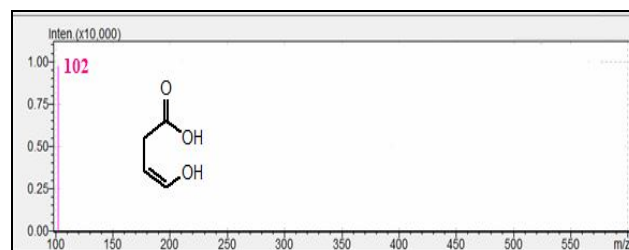
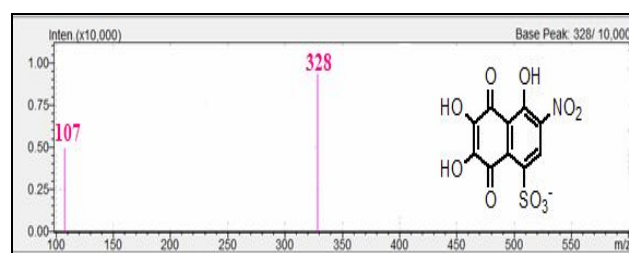
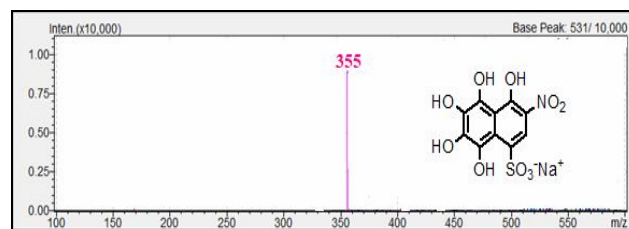


Fig. 8. LC/MS/MS spectra of carmoisine red solution after treatment by Electro-Fenton process.

Table 3 shows the three main compounds detected in the solution. After 60 min of treatment with the Electro-Fenton process, the intermediates of carmoisine red were identified: 4,6,7-Trihydroxy-3-nitro-5,8-dioxo-5,8-dihydro-naphthalene-1-sulfonic acid anion (*intermediate A*), Sodium; 4,5,6,7,8-pentahydroxy-3-nitro-naphthalene-1-sulfonate (*intermediate B*) and 4-Hydroxy-but-3-enoic acid (*intermediate C*).

Degradation pathway of carmoisine dye: LC-MS-MS was used to identify the intermediate compounds formed during the degradation of carmoisine red solution, allowing us to propose a schematic degradation pathway of carmoisine red by chemically generated hydroxyl radicals (Fig. 9).

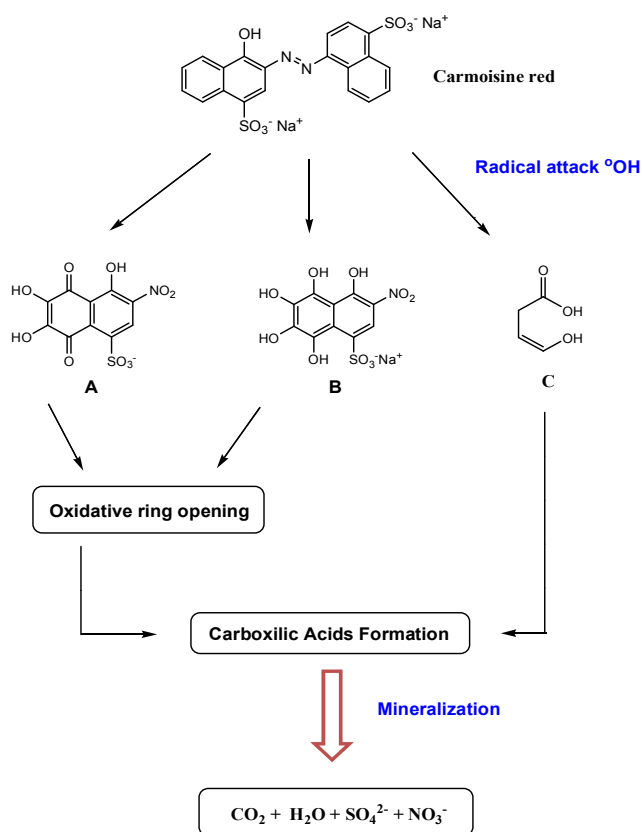


Fig. 9. Proposed degradation pathway of carmoisine red dye with Electro-Fenton process.

One of the main advantages of the Electro-Fenton process is the complete mineralization and degradation

of organic compounds. High-performance liquid chromatography coupled with mass spectroscopy HPLC/MS/MS and ionic chromatography analysis of electrolyzed azo dye revealed the formation of different oxidation products. The proposed reaction sequence for the degradation of dye carmoisine red is shown in Fig. 9. The oxidation of carmoisine red under the action of $\cdot\text{OH}$ started with the cleavage of the azo bond group $-\text{N}=\text{N}-$, the most active group in the structure of the dye molecule [38-40], to produce the naphthalene derivatives (A), (B) and 4-hydroxy-but-3-enoic acid compound. During the oxidation of organic molecules, most of the ions element went away from the dye structure as SO_3^- and N_xO_y ions. After that gradual cleavage of aromatic ring occurs, and this leads probably to the formation of CO_2 as the final product [41,42].

CONCLUSIONS

In this study, we have successfully applied the electro-Fenton process to the discoloration and degradation of 1 g l^{-1} carmoisine red in an aqueous solution. This system allows in situ production of Fenton's reagent and so the $\cdot\text{OH}$ via electrochemistry. To achieve optimal discoloration efficiency, carbon graphite (cathode) and platinum (anode) electrodes were used. The effects of parameters, namely Fe^{2+} concentration and electrolysis current were analyzed. The parameters determined to obtain an optimal 93% discoloration efficiency of carmoisine solution were $\text{pH} = 3$, electrolysis current 200 mA cm^{-2} , concentration of Fe^{2+} 0.2 mM and 60 min of electrolysis time.

Thereafter the degradation of carmoisine azo dye during Electro-Fenton treatment was analyzed by LC-MS-MS and ionic chromatography. It led to the formation of three aromatic intermediates: 4,6,7-trihydroxy-3-nitro-5,8-dioxo-5,8-dihydro-naphthalene-1-sulfonic acid anion; Sodium; 4,5,6,7,8-pentahydroxy-3-nitro-naphthalene-1-sulfonate; and 4-hydroxy-but-3-enoic acid. The sulfur atom of the azo dye (382 mg l^{-1}) was transformed to a sulphate SO_4^{2-} ions, with a concentration of 340 mg l^{-1} (89% of initial S), at the end of the treatment (300 min). A degradation pathway was proposed, in light of the obtained results. All these results show that the Electro-Fenton process is viable environmentally friendly technology for the remediation of

wastewaters containing dyes. Future work will be focused on the geometry of both electrodes materials and reactor in order to study the efficiency of the Electro-Fenton process.

REFERENCES

- [1] Wu, J.; Wang, T., Ozonation of aqueous azo dye in a semi-batch reactor. *Water Res.* **2001**, *35*, 1093-1099, DOI: [https://doi.org/10.1016/S0043-1354\(00\)00330-4](https://doi.org/10.1016/S0043-1354(00)00330-4).
- [2] Xuan, T.; Le, H.; Nguyen, T. Van; Zoungrana, L.; Avril, F.; Petit, E.; Mendret, J.; Bonniol, V.; Bechelany, M.; Lacour, S.; *et al.* Toxicity removal assessments related to degradation pathways of azo dyes: Toward an optimization of Electro-Fenton treatment. *Chemosphere* **2016**, *161*, 308-318, DOI: 10.1016/j.chemosphere.2016.06.108.
- [3] Robinson, T.; McMullan, G.; Marchant, R.; Nigam, P., Remediation of dyes in textile effluent: a critical review on current treatment technologies with a proposed alternative. *Bioresour. Technol.* **2001**, *77*, 247-255, DOI: [https://doi.org/10.1016/S0960-8524\(00\)00080-8](https://doi.org/10.1016/S0960-8524(00)00080-8).
- [4] Martínez-Huitle, C. A.; Brillas, E., Decontamination of wastewaters containing synthetic organic dyes by electrochemical methods: A general review. *Appl. Catal. B Environ.* **2009**, *87*, 105-145, DOI: 10.1016/j.apcatb.2008.09.017.
- [5] Naveenraj, S.; Solomon, R. V.; Venuvanalingam, P.; Asiri, A. M.; Anandan, S., Interaction between toxic azo dye C.I. Acid Red 88 and serum albumins. *J. Lumin.* **2013**, *143*, 715-722, DOI: 10.1016/j.jlumin.2013.06.012.
- [6] Erkurt, H. A., Biodegradation of Azo Dyes; **2010**; Vol. 9; ISBN 9783642118463.
- [7] Foroutan, R.; Mohammadi, R.; Farjadfard, S.; Esmaeili, H.; Ramavandi, B.; Sorial, G. A., Eggshell nano-particle potential for methyl violet and mercury ion removal: Surface study and field application. *Adv. Powder Technol.* **2019**, *30*, 2188-2199, DOI: 10.1016/j.apt.2019.06.034.
- [8] Brillas, E.; Mart, C. A.; Pii, H.; Brillas, E.; Mart, A., Decontamination of wastewaters containing synthetic organic dyes by electrochemical methods. *Appl. Catal. B Environ.* **2015**, *166*, 603-643, DOI: 10.1016/j.apcatb.2014.11.016.
- [9] Forgacs, E.; Cserháti, T.; Oros, G., Removal of synthetic dyes from wastewaters: a review. *Environ. Int.* **2004**, *30*, 953-71, DOI: 10.1016/j.envint.2004.02.001.
- [10] Santos, B.; Cervantes, F. J.; Lier, J. B., Van Review paper on current technologies for decolourisation of textile wastewaters: Perspectives for anaerobic biotechnology. *Bioresour. Technol.* **2007**, *98*, 2369-2385, DOI: 10.1016/j.biortech.2006.11.013.
- [11] Sales Solano, A. M.; Garcia-Segura, S.; Martínez-Huitle, C. A.; Brillas, E., Degradation of acidic aqueous solutions of the diazo dye Congo Red by photo-assisted electrochemical processes based on Fenton's reaction chemistry. *Appl. Catal. B Environ.* **2015**, *168-169*, 559-571, DOI: 10.1016/j.apcatb.2015.01.019.
- [12] Esmaeili, H.; Foroutan, R., Adsorptive behavior of methylene blue onto sawdust of sour lemon, date palm, and eucalyptus as agricultural wastes. *J. Dispers. Sci. Technol.* **2019**, *40*, 990-999, DOI: 10.1080/01932691.2018.1489828.
- [13] Meigoli Boushehrian, M.; Esmaeili, H.; Foroutan, R., Ultrasonic assisted synthesis of Kaolin/CuFe₂O₄ nanocomposite for removing cationic dyes from aqueous media. *J. Environ. Chem. Eng.* **2020**, *8*, 103869, DOI: 10.1016/j.jece.2020.103869.
- [14] Ruiz, E. J.; Hernández-ramírez, A.; Peralta-hernández, J. M.; Arias, C.; Brillas, E., Application of solar photoelectro-Fenton technology to azo dyes mineralization: Effect of current density, Fe²⁺ and dye concentrations. *Chem. Eng. J.* **2011**, *171*, 385-392, DOI: 10.1016/j.cej.2011.03.004.
- [15] Bai, L.; Fan, H.; Guo, X.; Yan, J.; Chen, Y. Treatment of microfiber alkali weight-reduction wastewater with high salt concentration by Fenton oxidation and bacterial degradation. *Water Environ. J.* **2019**, *34*, 0-3, DOI: 10.1111/wej.12527.
- [16] Brillas, E.; Sire, I.; Oturan, M. A., Electro-Fenton process and related electrochemical technologies based on Fenton's reaction chemistry. *Chem. Rev.* **2009**, *109*, 6570-6631, DOI: 10.1021/cr900136g.
- [17] Nidheesh, P. V.; Gandhimathi, R., Trends in electro-

- Fenton process for water and wastewater treatment: An overview. *Desalination* **2012**, *299*, 1-15, DOI: 10.1016/j.desal.2012.05.011.
- [18] Zhou, M.; Oturan, A.; Sirés, I., Electro-Fenton Process; **2018**; ISBN 9789811064050.
- [19] Harichandran, G.; Prasad, S., SonoFenton degradation of an azo dye, Direct Red. *Ultrason. Sonochem.* **2016**, *29*, 178-185, DOI: 10.1016/j.ultsonch.2015.09.005.
- [20] Pignatello, J. J., Dark and photoassisted Fe³⁺-catalyzed degradation of chlorophenoxy herbicides by hydrogen peroxide. *Environ. Sci. Technol.* **1992**, *26*, 944-951, DOI: 10.1021/jf00031a025.
- [21] Oturan, M.A.; Oturan, N.; Lahitte, C., Production of hydroxyl radicals by electrochemically assisted Fenton's reagent application to the mineralization of an organic micropollutant, pentachlorophenol. *J. Electroanal. Chem.* **2001**, *507*, 96-102, DOI: 10.1016/S0022-0728(01)00369-2.
- [22] Pérez, M.; Torrades, F.; Domènech, X.; Peral, J., Fenton and photo-Fenton oxidation of textile effluents. *Water Res.* **2002**, *36*, 2703-2710, DOI: 10.1016/S0043-1354(01)00506-1.
- [23] Özcan, A.; Oturan, M. A.; Oturan, N.; Yücel, S., Removal of acid orange 7 from water by electrochemically generated Fenton's reagent. *J. Hazard. Mater.* **2009**, *163*, 1213-1220, DOI: 10.1016/j.jhazmat.2008.07.088.
- [24] Neyens, E.; Baeyens, J., A review of classic Fenton's peroxidation as an advanced oxidation technique. *J. Hazard. Mater.* **2003**, *98*, 33-50, DOI: 10.1016/S0304-3894(02)00282-0.
- [25] Mansour, D., Mineralization of antibiotics by electro-Fenton process and by combined process electro-Fenton: biological treatment: application to the elimination of the industrial effluents' pollution, **2015**. *Ph.D. Thesis, The University of Rennes I*.
- [26] Zhang, H.; Fei, C.; Zhang, D.; Tang, F., Degradation of 4-nitrophenol in aqueous medium by electro-Fenton method. *J. Hazard. Mater.* **2007**, *145*, 227-232, DOI: 10.1016/j.jhazmat.2006.11.016.
- [27] Cardoso, N. F.; Pinto, R. B.; Lima, E. C.; Calvete, T.; Amavisca, C. V.; Royer, B.; Cunha, M. L.; Fernandes, T. H. M.; Pinto, I. S., Removal of remazol black B textile dye from aqueous solution by adsorption. *Desalination* **2011**, *269*, 92-103, DOI: 10.1016/j.desal.2010.10.047.
- [28] Fanchiang, J.; Tseng, D., Degradation of anthraquinone dye C.I. reactive blue 19 in aqueous solution by ozonation. *Chemosphere* **2009**, *77*, 214-221, DOI: 10.1016/j.chemosphere.2009.07.038.
- [29] Harisha, S.; Keshavayya, J.; Swamy, B.E.K.; Viswanath, C. C., Synthesis, characterization and electrochemical studies of azo dyes derived from barbituric acid. *Dye. Pigment.* **2017**, *136*, 742-753, DOI: 10.1016/j.dyepig.2016.09.004.
- [30] Siregar, C.; Martono, S.; Rohman, A., Application of Fourier transform infrared (FTIR) spectroscopy coupled with multivariate calibration for quantitative analysis of curcuminoid in tablet dosage form. *J. Appl. Pharm. Sci.* **2018**, *8*, 151-156, DOI: 10.7324/JAPS.2018.8821.
- [31] Muthukumar, M.; Karuppiyah, M. T.; Raju, G. B., Electrochemical removal of CI acid orange 10 from aqueous solutions. *Sep. Purif. Technol.* **2007**, *55*, 198-205, DOI: 10.1016/j.seppur.2006.11.014.
- [32] Özbay, N.; Yarg, A. F. J.; Yarbay-, R. Z. F.; Önal, E., Full factorial experimental design analysis of reactive dye removal by carbon adsorption. *J. Chem.* **2013**, 1-13, DOI: <https://doi.org/10.1155/2013/234904>.
- [33] Kolekar, Y. M.; Pawar, S. P.; Gawai, K. R.; Lokhande, P. D.; Shouche, Y. S.; Kodam, K. M., Decolorization and degradation of disperse blue 79 and acid orange 10, by bacillus fusiformis KMK5 isolated from the textile dye contaminated soil. *Bioresour. Technol.* **2008**, *99*, 8999-9003, DOI: 10.1016/j.biortech.2008.04.073.
- [34] Hu, C.; Yu, J. C.; Hao, Z.; Keung, P., Photocatalytic degradation of triazine-containing azo dyes in aqueous TiO₂ suspensions. *Appl. Catal. B Environ.* **2003**, *42*, 47-55.
- [35] Styliidi, M.; Kondarides, D. I.; Verykios, X. E., Visible light-induced photocatalytic degradation of acid orange 7 in aqueous TiO₂ suspensions. *Appl. Catal. B Environ.* **2004**, *47*, 189-201, DOI: 10.1016/j.apcatb.2003.09.014.
- [36] Thiam, A.; Sirés, I.; Centellas, F.; Cabot, P. L.; Brillas, E., Decolorization and mineralization of Allura Red AC azo dye by solar photoelectro-Fenton:

- Identification of intermediates. *Chemosphere* **2015**, *136*, 1-8, DOI: 10.1016/j.chemosphere.2015.03.047.
- [37] Stylidi, M.; Kondarides, D. I.; Verykios, X. E., Pathways of solar light-induced photocatalytic degradation of azo dyes in aqueous TiO₂ suspensions. *Appl. Catal. B Environ.* **2003**, *40*, 271-286. DOI: 10.1016/S0926-3373(02)00163-7.
- [38] Bandara, J.; Morrison, C.; Kiwi, J.; Pulgarin, C.; Peringer, P., Degradation/decoloration of concentrated solutions of orange II. Kinetics and quantum yield for sunlight induced reactions via Fenton type reagents. *J. Photochem. Photobiol. A Chem.* **1996**, *99*, 57-66, DOI: [https://doi.org/10.1016/1010-6030\(96\)04339-0](https://doi.org/10.1016/1010-6030(96)04339-0).
- [39] Ramirez, C.; Saldan, A.; Hernandez, B.; Acero, R.; Guerra, R.; Garcia-segura, S.; Brillas, E.; Peralta-herna, J. M., Electrochemical oxidation of methyl orange azo dye at pilot flow plant using BDD technology. *J. Ind. Eng. Chem.* **2013**, *19*, 571-579, DOI: 10.1016/j.jiec.2012.09.010.
- [40] Garcia-segura, S.; Brillas, E., Combustion of textile monoazo, diazo and triazo dyes by solar photoelectro-Fenton: Decolorization, kinetics and degradation routes. *Appl. Catal. B, Environ.* **2016**, *181*, 681-691, DOI: 10.1016/j.apcatb.2015.08.042.
- [41] Kayan, B.; Gözmen, B.; Demirel, M.; Gizir, A. M., Degradation of acid red 97 dye in aqueous medium using wet oxidation and electro-Fenton techniques. *J. Hazard. Mater.* **2010**, *177*, 95-102, DOI: 10.1016/j.jhazmat.2009.11.076.
- [42] Zheng, J.; Gao, Z.; He, H.; Yang, S.; Sun, C., Efficient degradation of acid orange 7 in aqueous solution by iron ore tailing Fenton-like process. *Chemosphere* **2016**, *150*, 40-48, DOI: 10.1016/j.chemosphere.2016.02.001.